REGIONAL PHOTOMETRIC MAPPING OF ASTEROID (101955) BENNU. D. R. Golish[1], J.-Y. Li[2], B. E. Clark[3], X.-D. Zou[2], J. L. Rizos[4], S. Fornasier[5,6], D. N. DellaGiustina[1], P. H. Hasselmann[5], C. A. Bennett[1], C. Drouet d'Aubigny[1], B. Rizk[1], M. G. Daly[7], O. S. Barnouin[8], J. A. Seabrook[7], L. Philpott[9], M. M. Al Asad[9], C. L. Johnson[9], B. Rozitis[10], A. Ryan[1], J. P. Emery[11], and D. S. Lauretta[1], [1]Lunar and Planetary Laboratory, University of Arizona (1415 N. 6th Ave., Tucson, AZ 85705, USA, dgolish@orex.lpl.arizona.edu), [2]Planetary Science Institute, Tucson, AZ, USA, [3]Department of Physics and Astronomy, Ithaca College, Ithaca, NY, USA, [4]Instituto de Astrofísica de Canarias, La Laguna, Tenerife, Spain, [5]LESIA, Observatoire de Paris, Université PSL, CNRS, Université de Paris, Sorbonne Université, 5 place Jules Janssen, 92195 Meudon, France, [6]Institut Universitaire de France (IUF), 1 rue Descartes, 75231 Paris CEDEX 05, France, [7]The Centre for Research in Earth and Space Science, York University, Toronto, Ontario, Canada, [8]The Johns Hopkins University Applied Physics Laboratory, Laurel, MD, USA [9]Department of Earth, Ocean and Atmospheric Sciences, University of British Columbia, Vancouver, British Columbia, Canada, [10]School of Physical Sciences, The Open University, Milton Keynes, UK, [11]Department of Astronomy and Planetary Science, Northern Arizona University, Flagstaff, AZ, USA

Introduction: The Origins, Spectral Interpretation, Resource Identification, and Security–Regolith Explorer (OSIRIS-REx) mission observed the surface of asteroid (101955) Bennu for ~2 years before sampling on 20 October 2020. A subset of those observations, acquired during the Detailed Survey phase [1], provided an expansive photometric dataset using all five filters of the MapCam imager [2]. Previously, we have published global empirical models based on these data [3], but those models treated Bennu's surface as uniform. However, from OSIRIS-REx's first resolved image of Bennu, it was clear that Bennu is heterogeneous. Its surface is dominated by boulders [4] with broad variation in albedo [5] and color [6].

Here we applied a regional analysis to that same photometric dataset, producing spatially variant photometric models of the surface. These models include the empirical models presented in the global study (Lommel-Seeliger, ROLO, Lunar-Lambert, Minnaert, and Akimov), as well as a new Hapke analysis.

Image Registration: Photometric backplanes (phase, incidence, and emission angle) from every image were calculated in ISIS3 [7]. To calculate the photometric angles accurately, the images were registered to the 20-cm ground sample distance (GSD) shape model derived from OSIRIS-REx Laser Altimeter (OLA) data [8]. However, the complete dataset, totaling over 4000 images, was too large and diverse to register to the shape model manually. Instead, we developed a registration method that utilized photometric and albedo simulations of every MapCam image to automatically register it to its own backplanes. With this method, we improved registration errors from 3–10 pixels (1–3 m), using a priori reconstructed SPICE pointing, to <1 pixel (<33 cm).

Empirical Modeling: To derive regional empirical photometric models, we binned the surface into 1°×1° latitude/longitude bins and solved each bin independently. As with the global analysis, we solved for disk functions separately from the phase functions.

To find the disk functions (Lommel-Seeliger, Minnaert, Lunar-Lambert, and Akimov) [3], we fit the reflectance data for every latitude/longitude bin with each model using a least squares minimization fitting routine. For the parameterized models, we solve for both global values and per-bin values of their free parameters. Despite a >4× increase in shape model resolution relative to the previous, global analysis, we observe significant scatter in the photometric data. Using regional disk function parameters improved the fits slightly, primarily because the spatially resolved analysis allows for albedo variation across the surface.

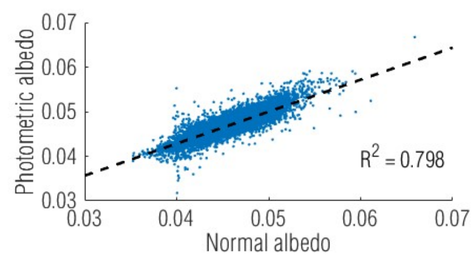

Figure 1. The photometric albedo derived from the linear phase function solution correlates with the independently derived normal albedo [5] of Bennu.

To solve for the phase functions (exponential, ROLO, Minnaert, and linear) [3], we disk-corrected the data for each latitude/longitude bin with each of the disk function solutions (global and regional) found in the previous step. We thus fit the phase functions against equigonal albedo, using the same least-squares fitting routines. Although ROLO includes explicit opposition surge terms, MapCam did not acquire any surface-resolved, low-phase images, thus we were unable to solve for those terms. We solved every combination of disk and phase function, for a total of 28 solutions (7 disk functions × 4 phase functions). The Minnaert model, for both disk and phase function, did not fit the surface well and typically had artifacts that followed Bennu's rough terrain. The exponential phase function was internally consistent, but resulted in albedos that were ~10% too high (compared with the PolyCam normal albedo map [5]) and had ~2× larger residuals. The ROLO and linear phase functions performed similarly, but linear had the best match to the global albedo map (Figure 1).

Photometric Mapping: With our spatially resolved photometric models, we were able to map regional photometric variations on Bennu's surface. The linear phase function depends on only one parameter (the phase slope, β), making it ideal for mapping. Phase slope is associated with albedo and roughness, where darker and rougher objects typically have steeper phase slopes (i.e., they become darker more quickly with increasing phase angle). Figure 2 (top) shows a map of phase slope, using a regional Akimov disk function, relative to Bennu's average phase slope $\beta \sim -0.023$). When compared with the albedo map (Figure 2, bottom) [5], there are clear correlations. Dark, rough areas such as Roc Saxum (–20°, 25°) and Tlanuwa Regio –30°, 270°) have ~25% steeper slopes than brighter, smoother areas such as the region at (–40°, 325°).

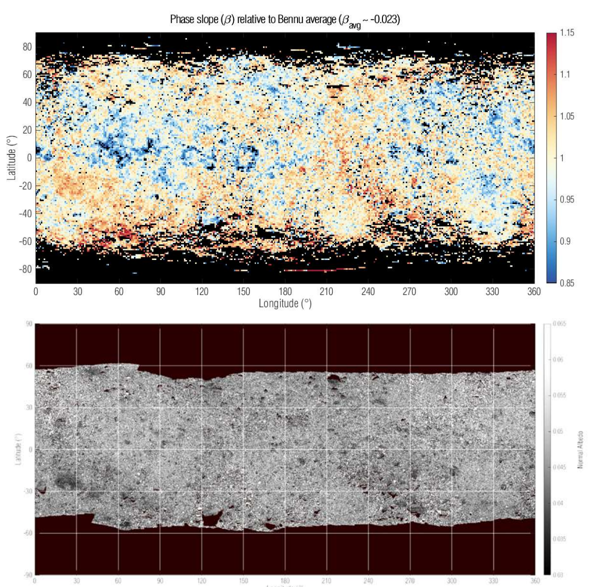

Figure 2. Maps of the linear phase slope β (top) and albedo [5] (bottom) demonstrate spatial correlations.

Disambiguating albedo and roughness, however, is challenging, as those characteristics tend to trend with each other on Bennu's surface [6]. Comparisons with other measures of roughness, such as thermal roughness derived from OSIRIS-REx Thermal Emission Spectrometer (OTES [9]) data and macroscopic roughness derived from OLA data, offer independent ways to correlate the photometric variation with Bennu's roughness.

Hapke Modeling: We also performed global and regional Hapke analyses [10] of Bennu's surface. Though we used Hapke's full roughness formulation, which notionally is designed to model sub-pixel surface variation, the model results were not statistically better than the empirical modeling. Nonetheless, we were able to model the surface regionally and produce maps of three Hapke parameters: the single-scattering albedo (SSA), asymmetry factor (ξ), and roughness (θ). SSA (Figure 3) and ξ follow albedo trends on Bennu closely, whereas θ shows less regional correlation.

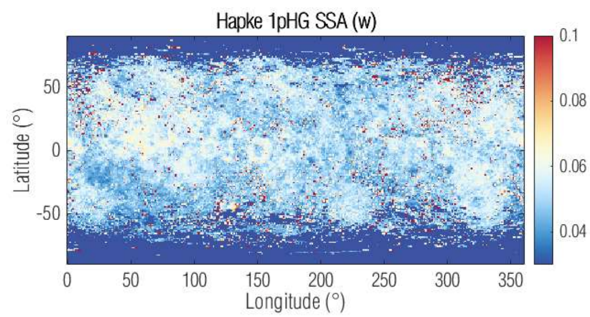

Figure 3. A map of single-scattering albedo from a regional Hapke analysis follow albedo trends on Bennu.

Acknowledgments: This work is supported by NASA under Contract NNM10AA11C issued through the New Frontiers Program. OLA and funding for the Canadian authors were provided by the Canadian Space Agency. This research has made use of the USGS Integrated Software for Imagers and Spectrometers (ISIS3). The image data are archived in the Planetary Data System Small Bodies Node at https://sbn.psi.edu/pds/resource/orex/.

References: [1] Lauretta, D. S. et al. (2017) *SSR*, 212, 925–984. [2] Rizk, B. et al. (2018) *SSR*, 214, 26. [3] Golish, D. R. et al. (2020) *Icarus*, 113724. [4] Lauretta, D. S. et al. (2019) *Nature,* 568, 55–60. [5] Golish, D. R. et al. (2021) *Icarus*, 114133. [6] DellaGiustina, D. G. et al. (2020) *Science,* 370(6517), eabc3660. [7] Keszthelyi, L. et al. (2013) *LPSC XLIV*, Abstract #2546. [8] Barnouin, O.S. et al. (2020) *PSS*, 180, 104764. [9] Rozitis, B. et al. (2020) *Sci. Adv*, 6 (41), eabc3699. [10] Hapke, B. (1984) *Icarus*, 59, 41-59.